JACS
JOURNAL OF THE AMERICAN CHEMICAL SOCIETY
Communication
pubs.acs.org/JACS

Solution-Processable Carbon Nanoelectrodes for Single-Molecule Investigations

Jingyuan Zhu,[†,‡] Joseph McMorrow,[†,‡] Rachel Crespo-Otero,[†] Geyou Ao,[∥] Ming Zheng,[∥] William P. Gillin,[§] and Matteo Palma*[,†]

[†]School of Biological and Chemical Sciences, Materials Research Institute, Institute of Bioengineering, and [§]Materials Research Institute and School of Physics and Astronomy, Queen Mary University of London, Mile End Road, London E1 4NS, United Kingdom

[∥]Materials Science and Engineering Division, National Institute of Standards and Technology, 100 Bureau Drive, Gaithersburg, Maryland 20899-8542, United States

Supporting Information

ABSTRACT: Here we present a solution-based assembly method for producing molecular transport junctions employing metallic single-walled carbon nanotubes as nanoelectrodes. The molecular junction conductance of a series of oligophenyls was successfully measured, highlighting the potential of an all-carbon based approach for the fabrication of solution-processable single-molecule junctions for molecular electronics.

We describe the assembly and electrical characterization of solution-processable molecular transport junctions (MTJs) fabricated employing metallic single-walled carbon nanotubes (SWCNTs) as nanoelectrodes. Due to the many potential benefits envisioned for molecular scale electronics, there has been significant effort in the fundamental understanding of metal-molecule-metal systems and their optoelectronic applications.[1−8] Different strategies have been developed to form MTJs, including scanning probe techniques, lithographic approaches, and mechanical/electromigration break junctions.[9−13] The use of carbon-based nanoelectrodes, in particular, has emerged as a promising approach[7,14−19] because of the intrinsic nanoscale size of CNTs and graphene and the reduced electronic mismatch granted by having molecules and electrodes of the same material (carbon atoms).[20,21]

Nevertheless, despite the substantial progress in single-molecule electronics from both fundamental and technological standpoints, challenges remain.[20] Principal among these are the time and cost involved in nanogap fabrication, the reliable control of the nanogap size, and the need for a facile (and scalable) technology for the establishment of electrical contact between individual molecules and metal electrodes.

Solution-based self-assembly methods represent a powerful approach to overcome the aforementioned limitations. Work in this context has typically focused on colloidal metallic nanoparticles as building blocks for fabricating nanogaps, that were then bridged to lithographically prefabricated electrodes.[8,22] A combination of top-down and bottom-up approaches has further been exploited by Bjørnholm et al. for the fabrication of gold nanorods as potential nanoelectrodes for single-molecule investigations.[23−25]

Herein we present a facile solution-based assembly method for producing MTJs by covalently linking metallic SWCNTs with electrically functional molecules. As a proof of principle, the single-molecule junction conductance of a series of oligophenyls was successfully measured. This work highlights the potential of an all-carbon-based approach for the fabrication of solution-processable single-molecule junctions for molecular electronics.

For our studies we employed DNA-wrapped SWCNTs[26] separated by chirality and electronic structure via a polymer aqueous two-phase separation method.[27−29] (DNA-assisted dispersion further leaves only the terminal ends of the SWCNTs available for direct functionalization.)[30] Building on our recent bottom-up assembly strategy for the formation of end-to-end CNT junctions,[30] we linked metallic single-chirality (7,4) SWCNTs in amidation reactions with three different diamine conjugated molecular linkers, containing 1, 2, and 3 phenyl rings [see the Supporting Information (SI)]. To confirm junction formation we cast low-coverage films on doped silicon wafer substrates coated with a hydrophobic layer (see the SI) shown to induce partial alignment of DNA-wrapped CNTs[31] and imaged them with atomic force microscopy (AFM).

The starting metallic SWCNTs before reaction had an average length of 473.7 ± 179.5 nm (see Figure SI-1). Figure 1 shows a representative AFM image of linear SWCNT junctions typically obtained employing *p*-phenylenediamine (PPD) as the molecular linker. The average length of the segments was found to be 838.3 ± 470.4 nm, strongly indicating the formation of molecular junctions. Similar behavior was found for the other two molecular linkers employed in this study: benzidine and 4,4″-diamino-*p*-terphenyl, which exhibited an average junction length of 1109.9 ± 546.6 and 1105.3 ± 569.1 nm, respectively (see Figures SI-2 and SI-3).[32,33]

Because of the small diameter of the SWCNTs employed in this study (∼8 Å), and due to steric hindrance effects, it is expected that only one molecule can bridge the nanotubes. Moreover, the presence of predominantly linear junctions, rather than branched, from all three linkers employed strongly indicates the presence of a single bridging molecule; two or more molecules would present multiple bindings sites that might

Received: November 18, 2015
Published: February 8, 2016

DOI: 10.1021/jacs.5b12086
J. Am. Chem. Soc. 2016, 138, 2905−2908

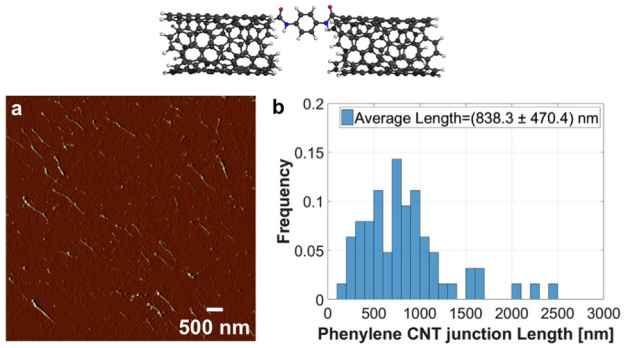

Figure 1. (Top) Schematic of a PPD-linked molecular junction. (a) AFM topographical image of molecular junctions formed using PPD as the molecular linker. (b) Normalized histogram showing the length distribution of the observed molecular junctions. The average length of 838.3 ± 470.4 nm was determined from ~100 nanotubes.

induce the formation of branched CNT junctions. To further confirm the presence of predominantly one molecule between SWCNTs in the junctions, we carried out density functional theory (DFT) calculations at PBE0-D3/SV(P) level of theory considering water as the solvent (COSMO model)[34−37] (see the SI). Our calculations show that the formation of linear junctions where two molecules bridge two nanotubes is energetically less favorable than the junctions with one bridging molecule (see Figures 2 and SI-7−9). A second molecule in the junction

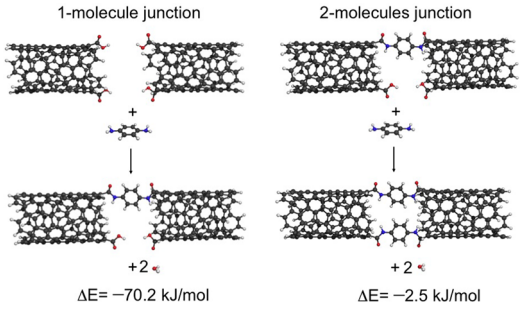

Figure 2. Reactions of formation for linear junctions with one and two bringing molecules. The energies were obtained at PBE0-D3/SV(P) level of theory considering water as the solvent (COSMO model).

induces a significant strain, increasing the energy of formation by ~68 kJ/mol.[38] At the same time, the entropy decreases because of the restrictions to rotations and vibrations induced by the second molecule. Therefore, the formation of SWCNT junctions linked by two molecules is unlikely to occur. These findings allow us to reasonably assume that we are assembling predominately single-molecule junctions.

To investigate the electrical properties of the MTJs assembled in this study, we measured their current−voltage (I−V) characteristics as a function of the distance between a metallic AFM tip used as a mobile electrode and a fixed macroscopic metal electrode (see Figure 3 and the SI). This approach[25,39,40] allowed us to record force-controlled I−V responses (in PeakForce TUNA mode, Bruker) at different locations along individual SWCNT molecular junctions.

Figure 3a shows a representative conductive AFM[41] image of a PPD-SWCNT junction. The substrates were subject to cleaning procedures (see the SI) in order to eliminate salt residues from the buffer solution and to facilitate the removal of the DNA wrapped around the tubes, as they could affect the electronic

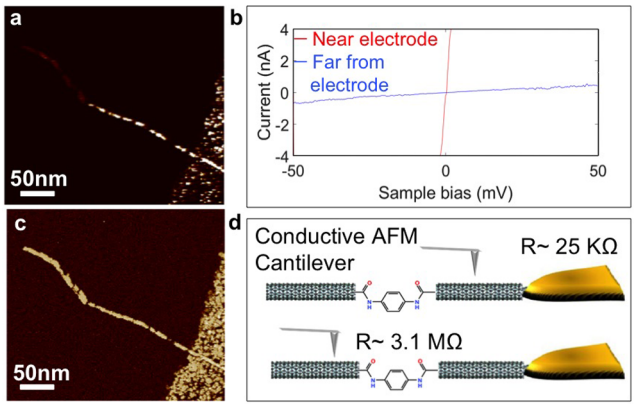

Figure 3. (a) Representative conductive AFM image of a MTJ formed using PPD as the molecular linker and interfaced to a macroscopic metal electrode. (b) Representative I−V curves recorded at selected points across the MTJ: red line for measurements in close proximity to the macroscopic electrode and blue line for measurements at the far end from the macroscopic electrode. (c) Phase AFM image of the MTJ shown in (a). (d) Schematic of the conductive AFM measurements on the MTJs.

properties of the nanotubes. The contact resistance of the SWCNT was determined by acquiring I−V curves in close proximity to the macroscopic electrode (between 30 and 120 nm, see Figure 3b and schematic in Figure 3d). We determined in this way a resistance (R) of ~25 KΩ that is the typical contact resistance for single SWCNTs using metal contacts.[40,42] We did not observe any noticeable increase in resistance along the nanotube within this distance range, as indeed expected for short SWCNTs.[40] On repeating the measurements along the same SWCNT we obtained the same R within a 4% error, indicating that the AFM tip did not damage the SWCNT surface.

To determine the junction resistance, we measured I−V characteristics of the MTJ at the far end from the macroscopic electrode (see schematic in Figure 3d). The junction resistances were determined from the inverse slope of the I−V curves recorded in the linear region, which was between −50 and 50 mV (see Figure 3b and the SI). Employing this approach, we determined a resistance of ~3.1 MΩ for individual PPD-SWCNT junctions. This significant increase in the measured resistance across the MTJ (from KΩs to MΩs) is in line with the expected presence of a PPD molecule bridging SWCNT segments. In a similar way, we measured the resistance of SWCNT junctions formed with benzidine and 4,4″-diamino-*p*-terphenyl linkers (see the SI).

The resistance values were plotted in histograms in semilog scale, and the peaks were fit to Gaussians (see Figures SI-10−12).[43] The center values were then taken as the junction resistances.[44] From the inverse of these values we determined the molecular junctions conductances of the SWCNT-based MTJs. Table 1 summarizes our results. The average conductance values for the three oligophenyls are in good agreement with the literature values.[45]

The measured conductance decays exponentially with molecular length. The tunneling decay constant β can be estimated making use of the equations typically employed to describe nonresonant tunneling:[46,47] $G = G_c \exp(-\beta L)$ or $R = R_c \exp(\beta L)$. Here G_c (R_c) is an effective contact conductance (resistance) of the molecular wire junction, while β is the tunneling decay constant, and L the tunneling distance taken to be the length of the molecule.[48]

DOI: 10.1021/jacs.5b12086
J. Am. Chem. Soc. 2016, 138, 2905−2908

Table 1. Molecular Linkers Employed and Measured Molecular Junction Conductance Values

molecule	conductance (G_0)
PPD	$8.0 \times 10^{-3} \pm 2.4 \times 10^{-3}$
benzidine	$1.4 \times 10^{-3} \pm 5.5 \times 10^{-4}$
terphenyl	$1.8 \times 10^{-4} \pm 4.2 \times 10^{-5}$

Figure 4 shows the plot of junction conductance vs molecular length for the series of oligophenyls employed in our

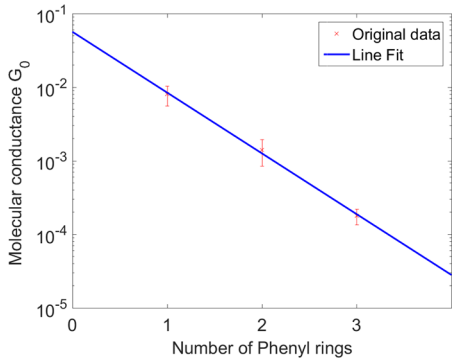

Figure 4. Measured conductances of oligophenyl SWCNT-based MTJs plotted against number of phenyl rings.

investigations, i.e., with 1−3 phenyl rings. The plot fits an exponential form with an estimated decay constant of 0.5 Å^{-1}, i.e., 1.9 per phenyl ring. This result is in reasonable agreement with the values of ∼1.8[46] and ∼1.7[45,49] per phenyl ring measured in metal-molecule-metal junctions via scanning probe-based techniques. Moreover, this is further evidence for tunneling conductance through the aromatic rings employed in our SWCNT-based MTJs.[50]

Extrapolating the plot fit (for R) to zero length, we can further estimate the contact resistance of the SWCNT-molecule-SWCNT junctions to be ∼108 KΩ (see Figure SI-13), i.e., comparable to the contact resistance found for Au-molecule-Au junctions (∼360 KΩ).[49] This value indicates that the molecule-SWCNT coupling is rather strong, as expected for amide bonds linkages that possess a partial double-bond character.

In conclusion, we have presented a strategy for the fabrication of solution-processable MTJs that employ molecular building blocks assembled between metallic CNT electrodes. The molecular conductance of a series of oligophenyls was measured, and the average values were found to be in line with the literature values. The main advantage and novelty of the approach presented here is the low-cost/simplicity of integration via assembly in (aqueous-based) solution. To our knowledge, this is the first example of solution-processable carbon-based MTJs. We anticipate that this new method of fabricating MTJs will be employed to produce a variety of solution-processable nano-electronic devices.

■ ASSOCIATED CONTENT

Supporting Information

The Supporting Information is available free of charge on the ACS Publications website at DOI: 10.1021/jacs.5b12086.

Experimental procedures, AFM images, data analysis and DFT calculations (PDF)

■ AUTHOR INFORMATION

Corresponding Author

*m.palma@qmul.ac.uk

Author Contributions

‡These authors contributed equally.

Funding

No competing financial interests have been declared.

Notes

The authors declare no competing financial interest.

■ ACKNOWLEDGMENTS

We gratefully acknowledge financial support from the Engineering and Physical Sciences Research Council under Award EP/M029506/1. J.Z. is financially supported by the Chinese Scholarship Council. We thank Khaled Kaja (Bruker) for helpful discussions and technical support.

■ REFERENCES

(1) Heath, J. R. *Annu. Rev. Mater. Res.* **2009**, *39*, 1.
(2) Ratner, M. *Nat. Nanotechnol.* **2013**, *8*, 378.
(3) Tao, N. J. *Nat. Nanotechnol.* **2006**, *1*, 173.
(4) Lindsay, S. M.; Ratner, M. A. *Adv. Mater.* **2007**, *19*, 23.
(5) Moth-Poulsen, K.; Bjornholm, T. *Nat. Nanotechnol.* **2009**, *4*, 551.
(6) Focus Issue: *Nat. Nanotechnol.* **2013**, *8*, 377.10.1038/nnano.2013.116
(7) Jia, C. C.; Guo, X. F. *Chem. Soc. Rev.* **2013**, *42*, 5642.
(8) Sun, L.; Diaz-Fernandez, Y. A.; Gschneidtner, T. A.; Westerlund, F.; Lara-Avila, S.; Moth-Poulsen, K. *Chem. Soc. Rev.* **2014**, *43*, 7378.
(9) Shen, Q.; Guo, X. F.; Steigerwald, M. L.; Nuckolls, C. *Chem. - Asian J.* **2010**, *5*, 1040.
(10) Perrin, M. L.; Burzuri, E.; van der Zant, H. S. J. *Chem. Soc. Rev.* **2015**, *44*, 902.
(11) Aradhya, S. V.; Venkataraman, L. *Nat. Nanotechnol.* **2013**, *8*, 399.
(12) Diez-Perez, I.; Hihath, J.; Hines, T.; Wang, Z. S.; Zhou, G.; Mullen, K.; Tao, N. J. *Nat. Nanotechnol.* **2011**, *6*, 226.
(13) Xiang, D.; Jeong, H.; Kim, D.; Lee, T.; Cheng, Y. J.; Wang, Q. L.; Mayer, D. *Nano Lett.* **2013**, *13*, 2809.
(14) Guo, X.; Small, J. P.; Klare, J. E.; Wang, Y.; Purewal, M. S.; Tam, I. W.; Hong, B. H.; Caldwell, R.; Huang, L.; O'Brien, S.; Yan, J.; Breslow, R.; Wind, S. J.; Hone, J.; Kim, P.; Nuckolls, C. *Science* **2006**, *311*, 356.
(15) Feldman, A. K.; Steigerwald, M. L.; Guo, X. F.; Nuckolls, C. *Acc. Chem. Res.* **2008**, *41*, 1731.
(16) Cao, Y.; Dong, S. H.; Liu, S.; Liu, Z. F.; Guo, X. F. *Angew. Chem., Int. Ed.* **2013**, *52*, 3906.
(17) Marquardt, C. W.; Grunder, S.; Blaszczyk, A.; Dehm, S.; Hennrich, F.; von Lohneysen, H.; Mayor, M.; Krupke, R. *Nat. Nanotechnol.* **2010**, *5*, 863.
(18) Cao, Y.; Dong, S. H.; Liu, S.; He, L.; Gan, L.; Yu, X. M.; Steigerwald, M. L.; Wu, X. S.; Liu, Z. F.; Guo, X. F. *Angew. Chem., Int. Ed.* **2012**, *51*, 12228.
(19) Thiele, C.; Vieker, H.; Beyer, A.; Flavel, B. S.; Hennrich, F.; Torres, D. M.; Eaton, T. R.; Mayor, M.; Kappes, M. M.; Golzhauser, A.; Lohneysen, H. V.; Krupke, R. *Appl. Phys. Lett.* **2014**, *104*, 103102.
(20) van der Molen, S. J.; Naaman, R.; Scheer, E.; Neaton, J. B.; Nitzan, A.; Natelson, D.; Tao, N. J.; van der Zant, H.; Mayor, M.; Ruben, M.; Reed, M.; Calame, M. *Nat. Nanotechnol.* **2013**, *8*, 385.
(21) Yan, H. J.; Bergren, A. J.; McCreery, R. L. *J. Am. Chem. Soc.* **2011**, *133*, 19168.
(22) Jain, T.; Tang, Q. X.; Bjornholm, T.; Norgaard, K. *Acc. Chem. Res.* **2014**, *47*, 2.
(23) Tang, Q. X.; Tong, Y. H.; Jain, T. T.; Hassenkam, T.; Wan, Q.; Moth-Poulsen, K.; Bjornholm, T. *Nanotechnology* **2009**, *20*, 245205.
(24) Jain, T.; Lara-Avila, S.; Kervennic, Y. V.; Moth-Poulsen, K.; Norgaard, K.; Kubatkin, S.; Bjornholm, T. *ACS Nano* **2012**, *6*, 3861.
(25) Hassenkam, T.; Moth-Poulsen, K.; Stuhr-Hansen, N.; Norgaard, K.; Kabir, M. S.; Bjornholm, T. *Nano Lett.* **2004**, *4*, 19.

DOI: 10.1021/jacs.5b12086
J. Am. Chem. Soc. 2016, 138, 2905−2908

(26) Zheng, M.; Jagota, A.; Semke, E. D.; Diner, B. A.; Mclean, R. S.; Lustig, S. R.; Richardson, R. E.; Tassi, N. G. *Nat. Mater.* **2003**, *2*, 338.
(27) Tu, X. M.; Manohar, S.; Jagota, A.; Zheng, M. *Nature* **2009**, *460*, 250.
(28) Ao, G. Y.; Khripin, C. Y.; Zheng, M. *J. Am. Chem. Soc.* **2014**, *136*, 10383.
(29) Ao, G.; Zheng, M. *Current protocols in chemical biology* **2015**, *7*, 43.
(30) Palma, M.; Wang, W.; Penzo, E.; Brathwaite, J.; Zheng, M.; Hone, J.; Nuckolls, C.; Wind, S. J. *J. Am. Chem. Soc.* **2013**, *135*, 8440.
(31) McLean, R. S.; Huang, X. Y.; Khripin, C.; Jagota, A.; Zheng, M. *Nano Lett.* **2006**, *6*, 55.
(32) As previously demonstrated (see ref 30): To verify that an amidation reaction and not a supramolecular interaction is actually responsible for the formation of SWCNT junctions, we measured the length of the SWCNTs after addition of the diamine molecular linker/s without the amide coupling and activating agents (Sulfo-NHS and EDCI). The average nanotube length in this case was comparable to that of the pristine SWCNTs, thus indicating that the amidation reaction is the main driving force for the formation of SWCNT junctions (see Figures SI-4 and SI-5). Moreover, we characterized the length of our SWCNTs when a 4,4-toluenesulfonyl molecular linker was employed for junction formation. As clearly shown by the AFM image and the histogram of length distribution in Figure SI-6, when employing a phenyl linker without any amine end-groups, the average length of the SWCNTs is comparable to the length of pristine SWCNTs. This result further indicates that the amidation reaction is the main driving force towards the formation of the SWCNTs junctions, and we can rule out noncovalent binding.
(33) The overall yield of junction formation, defined as the number of nanostructures longer than 900 nm, was estimated to be ~70%.
(34) Adamo, C.; Barone, V. *J. Chem. Phys.* **1999**, *110*, 6158.
(35) Grimme, S.; Antony, J.; Ehrlich, S.; Krieg, H. *J. Chem. Phys.* **2010**, *132*, 154104.
(36) Klamt, A.; Schuurmann, G. *J. Chem. Soc., Perkin Trans. 2* **1993**, 799.
(37) Schäfer, A.; Horn, H.; Ahlrichs, R. *J. Chem. Phys.* **1992**, *97*, 2571.
(38) This value was obtained for the most stable junction configuration, i.e., the linear configuration at PBE-D3/SV(P) level of theory (see the SI).
(39) Loiacono, M. J.; Granstrom, E. L.; Frisbie, C. D. *J. Phys. Chem. B* **1998**, *102*, 1679.
(40) Gomez-Navarro, C.; De Pablo, P. J.; Gomez-Herrero, J.; Biel, B.; Garcia-Vidal, F. J.; Rubio, A.; Flores, F. *Nat. Mater.* **2005**, *4*, 534.
(41) Mativetsky, J. A.; Palma, M.; Samori, P. *Top. Curr. Chem.* **2008**, *285*, 157.
(42) Javey, A.; Guo, J.; Wang, Q.; Lundstrom, M.; Dai, H. J. *Nature* **2003**, *424*, 654.
(43) An additional control experiment was perfromed by measuring the resistance of SWCNT junctions formed with hexamethylenediamine (HMD) as the molecular linker, i.e., employing a nonconjugated molecule. The resistance for HMD-based junctions was found to be $1.12 \times 10^8 \pm 6.16 \times 10^7$ Ω (see Figure SI-14). This value is in good agreement with the literature value of $\sim 10^8$ Ω obtained for hexanethiol monolayers in nanoparticle bridges (see the SI).
(44) Mativetsky, J. M.; Pace, G.; Elbing, M.; Rampi, M. A.; Mayor, M.; Samori, P. *J. Am. Chem. Soc.* **2008**, *130*, 9192.
(45) Venkataraman, L.; Klare, J. E.; Nuckolls, C.; Hybertsen, M. S.; Steigerwald, M. L. *Nature* **2006**, *442*, 904.
(46) Wold, D. J.; Haag, R.; Rampi, M. A.; Frisbie, C. D. *J. Phys. Chem. B* **2002**, *106*, 2813.
(47) Ratner, M. A.; Davis, B.; Kemp, M.; Mujica, V.; Roitberg, A.; Yaliraki, S. *Ann. N. Y. Acad. Sci.* **1998**, *852*, 22.
(48) For a conjugated molecule, through-bond tunneling along the molecular backbone is expected to dominate over through-space tunneling.
(49) Kim, T.; Liu, Z. F.; Lee, C.; Neaton, J. B.; Venkataraman, L. *Proc. Natl. Acad. Sci. U. S. A.* **2014**, *111*, 10928.
(50) Mobile counterions associated with the DNA do not dominate charge transport through linked SWCNTs: Mobile counterions would be relevant for measurements in solution, while we work in dry/air.

DOI: 10.1021/jacs.5b12086
J. Am. Chem. Soc. 2016, 138, 2905−2908